Applied Catalysis A: General 492 (2015) 127–132

Contents lists available at ScienceDirect

Applied Catalysis A: General

journal homepage: www.elsevier.com/locate/apcata

Promoting effect of Al on tethered ligand-modified Rh/SiO_2 catalysts for ethylene hydroformylation

Jia Liu[a,c], Li Yan[a], Yunjie Ding[a,b,*], Miao Jiang[a,c], Wenda Dong[a,c], Xiangen Song[a], Tao Liu[a], Hejun Zhu[a]

[a] Dalian National Laboratory for Clean Energy, Dalian Institute of Chemical Physics, Chinese Academy of Sciences, Dalian 116023, China
[b] State Key Laboratory of Catalysis, Dalian Institute of Chemical Physics, Chinese Academy of Sciences, Dalian 116023, China
[c] University of Chinese Academy of Sciences, Beijing 100039, China

ARTICLE INFO

Article history:
Received 11 June 2014
Received in revised form 3 December 2014
Accepted 5 December 2014
Available online 12 December 2014

Keywords:
Rhodium
Al
Tethered phosphine
Ethylene
Hydrofromylation

ABSTRACT

A Rh/SiO_2 catalyst with excellent activity and stability for ethylene hydroformylation was developed by modifying with tethered diphenylphosphinopropyl and doped with an Al promoter. The catalyst was characterized by means of N_2 adsorption/desorption isotherms, transmission electron microscope, NH_3 temperature programmed desorption, Fourier transform infrared spectroscopy and solid-state nuclear magnetic resonance. Experimental results showed that the existence of the Al promoter inhibited the growth of Rh particles, increased the number of exposed Rh atoms, changed the acidity of the catalyst surface, promoted in situ formation of active species that were similar to their corresponding homogeneous counterparts, and enhanced electron density of the P atom in the phosphine ligand.

1. Introduction

Hydroformylation of alkenes to produce aldehydes is a reaction of significant interest for researchers of both academic and industrial sectors [1], and several generations of catalysts have already been developed by researchers. Though traditional catalysts are categorized into homogeneous and heterogeneous, till now, only homogeneous catalysts are used in most hydroformylation industrial processes due to the advantages of high activity and mild reaction conditions. However, heterogeneous catalysts have the advantage of easy separation from reactants and products, which is the drawback of the homogeneous catalysts. To combine the advantages of the homogeneous and heterogeneous catalysts, researchers have devoted great efforts to develop new catalytic systems, especially immobilization or heterogenization of active transition-metal complex on solid supports [2,3]. However, these systems suffer from low stability because of the leaching of active species [4,5]. We have reported previously a new tethered ligand-modified Rh/SiO_2 catalyst in which the phosphine ligands as well as the Rh particles were anchored on the surface of the support to avoid the leaching of the active species [6]. The tethered ligand-modified Rh/SiO_2 catalyst showed an excellent stability, but the activity needed to be improved.

Since doping with inorganic promoters is a traditional strategy to modify catalysts in heterogeneous catalysis and the Rh element is by far the most efficient metal for hydroformylation of olefins, accordingly, many additives, such as Zn [7], Mo [8,9], Ag [10] and Se [11], have been investigated to improve the activity of the Rh/SiO_2 catalyst, and they have been reported to increase the activity of the catalyst for the hydroformylation reaction by decreasing the size of the Rh nano-particles or to modify the electronic properties of the Rh nano-particles. Al_2O_3 is one of the most used inorganic oxide supports, and investigators have reported many modified Rh/Al_2O_3 catalysts, such as Rh/nano-Al_2O_3 [12], modified $Rh/SiO_2{\cdot}Al_2O_3$ [13] and Rh complexes/Al_2O_3-ZrO_2 [14], for the hydroformylation of olefins. Lenarda et al. have reported a Rh/Al on silica system used for catalyzing propylene hydroformylation [15]. However, these traditional heterogeneous catalysts still suffered from poor activity and/or selectivity for the hydroformylation of olefins.

In this work, by taking the advantage of the promoter effect in heterogeneous catalysis, we introduced Al as an inorganic promoter to improve the activity of an Rh/SiO_2 catalyst modified with tethered diphenylphosphinopropyl. The objective of this work is to explore a new approach for improving the activity of

* Corresponding author at: Dalian National Laboratory for Clean Energy, Dalian Institute of Chemical Physics, Chinese Academy of Sciences, Dalian 116023, China. Tel.: +86 41184379143; fax: +86 41184379143.
E-mail address: dyj@dicp.ac.cn (Y. Ding).

http://dx.doi.org/10.1016/j.apcata.2014.12.011
0926-860X/

ligand-modified Rh catalysts. To our knowledge, no work has been done with inorganic promoters on ligand-modified Rh catalysts until now. The catalysts were tested in the ethylene hydroformylation reaction and characterized by means of N_2 adsorption/desorption isotherms, transmission electron microscope (TEM), NH_3 temperature programmed desorption (NH_3-TPD), Fourier transform infrared spectroscopy (FT-IR) and solid-state nuclear magnetic resonance (solid-state NMR).

2. Experimental

2.1. Catalyst preparation

$RhAl_n/SiO_2$ was prepared by co-impregnation of silica gel with $RhCl_3{\cdot}xH_2O$ and $Al(NO_3)_3{\cdot}9H_2O$ in ethanol and dried in air. Subsequently, it was calcined at 573 K for 4 h and then reduced in a H_2 flow at 573 K for 4 h at atmospheric pressure. After washing off the Cl^-, it was reduced again at 573 K and restored in an Ar atmosphere. The metal loading of Rh was 1.2 wt%, and the atom ratio of Al to Rh was n (n = 0.2, 1, 3). The Rh/SiO_2 catalyst was prepared in the same way without the addition of the $Al(NO_3)_3{\cdot}9H_2O$.

3-Diphenylphosphinopropyltriethoxysilane (DPPPTS) was prepared according to the literature [16]. 0.9521 g lithium was cut into pieces and added to a solution of 10.0183 g diphenylchlorophosphine in 40 ml tetrahydrofuran with magnetic stirring. An exothermic reaction took place instantly, and the color of the solution turned red-brown with a great deal of precipitation. The mixture was stirred for 12 h and then filtered. The filtrate was added dropwise to a solution of 15.3727 g 3-chloropropyltriethoxysilane in 45 ml tetrahydrofuran at room temperature. The solution was stirred for 18 h. Most of the tetrahydrofuran was removed by distillation. The produced precipitate was filtered off and the filtrate was distilled at reduced pressure. A light yellow liquid was obtained at 300 Pa, 459–461 K. ^{31}P NMR ($CDCl_2$): δ −17.2 ppm.

Tethered diphenylphosphinopropyl/modified Rh/SiO_2 and $RhAl_n/SiO_2$ catalysts were prepared as described in literature [6]. In the case of the DPPPTS-$RhAl_n/SiO_2$, 0.3 g $RhAl_n/SiO_2$ was added to a solution of 0.03 g DPPPTS in 3 ml toluene, the mixture was stirred for 16 h at room temperature and then for another 6 h under reflux. After cooling to room temperature, the toluene was removed by vacuum-pumping for 3 h. The DPPPTS-Rh/SiO_2 had the same P/Rh ratio with the DPPPTS-$RhAl_n/SiO_2$.

All manipulations referring to the use of DPPPTS were carried out under an argon atmosphere.

2.2. Ethylene hydroformylation

The hydroformylation of ethylene was performed in a continuous flow fixed-bed reactor with inner diameter of 4.6 mm under the condition of $P(C_2H_4{:}CO{:}H_2)$ = 1:1:1) = 1.0 MPa, T = 393 K, $m_{catalyst}$ = 0.3 g, GHSV = 2000 h^{-1}, and P/Rh = 2.2. The effluent passed through a condenser filled with 70 ml de-ionized water. The so-obtained aqueous solution was analyzed by a HP-6890N GC with an FFAP column, using an FID detector and with ethanol as an internal standard. The tail gas was analyzed on-line using the same HP-6890N GC with a Porapak-QS column and a TCD detector. The turn-over-frequency (TOF) of the catalyst was calculated based on the Rh content of the catalyst.

2.3. Characterization

N_2 adsorption–desorption isotherms of the samples were measured using a Quantachrome Autosorb-1 instrument. Prior to the measurements, the samples were degassed under vacuum at 573 K for 3 h.

The morphology of the catalysts was observed using an FEI Tecnai G^2 F30 S-Twin instrument. The Rh particle size statistics was completed by using the software (Nano Measurer 1.2).

FT-IR spectra were recorded on a Bruker Tensor 27 instrument. The liquid samples were deposited onto a KBr window and the solid samples were pressed into self-supporting discs of the same amount and placed in an IR cell. The samples prepared for measuring pyridine FT-IR spectra were treated under vacuum at 573 K for 0.5 h. Then, they were exposed to pyridine vapor for 0.5 h at room temperature, followed by vacuuming. After 30 min, the spectra were recorded. The vacuuming was a prerequisite for the subsequent operation and would not be mentioned specifically. Then the temperature was raised to 423 K and held for 0.5 h. After cooling to room temperature, the spectra were collected. The spectra at 523 K were obtained after a new turn of temperature rise, retention and descent. The samples prepared for recording in situ FT-IR spectra were treated as follows: reduction in a H_2 flow for 1 h at 393 K, adsorption of a $CO{:}H_2$ = 1:1 mixture gas for 0.5 h at 323 K, then purging with N_2 for 0.5 h at 323 K.

NH_3-TPD was performed using a Micromeritics AutoChem 2910 instrument. After treating at 573 K for 0.5 h, the samples were cooled to 373 K and adsorbed NH_3 to saturation in a He flow. Then the temperature was raised to 573 K at a rate of 10 K min^{-1} along with the detection of NH_3.

Solid state ^{31}P NMR spectra and ^{27}Al NMR spectra were acquired using a VARIAN infinity plus spectrometer. ^{31}P chemical shifts were referenced to the chemical shift of H_3PO_4 at 0 ppm, while ^{27}Al chemical shifts were referenced to the chemical shift of $[Al(H_2O)_6]$ at 0 ppm.

3. Results and discussion

3.1. Hydroformylation of ethylene

The catalytic performances of ethylene hydroformylation over the DPPPTS-$RhAl_n/SiO_2$ and DPPPTS-Rh/SiO_2 catalysts were evaluated from the TOF versus time on stream, as shown in Fig. 1. All catalysts exhibited far higher activities than the conventional heterogeneous Rh/SiO_2 catalyst (TOF = 0.8 h^{-1}). As there was an induction period for the ligand-modified Rh catalyst to form in situ the active species, the catalytic activities of all catalysts increased with a prolonged time during the first 144 h, and then became steady. Under identical reaction conditions, the DPPPTS-$RhAl_n/SiO_2$ catalysts showed much higher activities than the DPPPTS-Rh/SiO_2

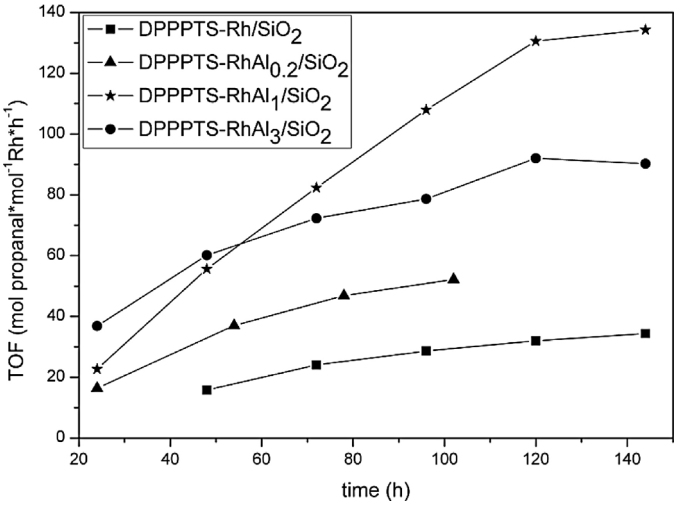

Fig. 1. Catalytic performance of ethylene hydroformylation over DPPPTS-Rh/SiO_2 and DPPPTS-$RhAl_n/SiO_2$.

Table 1
Texture properties of catalysts.

Sample	S_{BET}[a] (m^2/g)	Average D_p[b] (nm)	V_p[c] (cm^3/g)
DPPPTS-$RhAl_1/SiO_2$	217	13.3	0.72
DPPPTS-Rh/SiO_2	205	12.7	0.65

[a] BET surfaces.
[b] Average pore diameters.
[c] Pore volumes of the samples.

catalyst. Furthermore, the amount of Al played an important role in the activity of the DPPPTS-$RhAl_n/SiO_2$ catalysts. TOFs increased when n increased from 0.2 to 1 and then decreased when n increased up to 3. Thus, it was suggested that appropriate mole ratio of Al to Rh should be 1. The TOFs at a time-on-stream of 144 h of the DPPPTS-$RhAl_1/SiO_2$ sample ($134\ h^{-1}$) was about 4 times higher than that of the DPPPTS-Rh/SiO_2 ($34\ h^{-1}$) catalyst. It is noticeable that the activity of DPPPTS-$RhAl_1/SiO_2$ was higher than DPPPTS-Rh/SiO_2 due to the doping of the Al promoter, therefore, we made a detailed investigation on the promoting effect of Al between the DPPPTS-$RhAl_1/SiO_2$ and DPPPTS-Rh/SiO_2 catalysts.

3.2. Nitrogen adsorption/desorption isotherms

N_2 adsorption/desorption isotherms was used to investigate the texture properties of the two catalysts (Table 1). The DPPPTS-$RhAl_1/SiO_2$ had slightly higher S_{BET}, average D_p and V_p values than the DPPPTS-Rh/SiO_2. Since the two catalysts did not show much difference in pore structure and pore diameter distribution, the promoting effect of Al in the texture properties of the catalysts could be ignored.

3.3. TEM

In order to study the promoting effect of Al on the performance of the DPPPTS-Rh/SiO_2 catalyst, the distributions of the Rh nanoparticle size in Rh/SiO_2 and $RhAl_1/SiO_2$ were calculated on the basis of the TEM images. The TEM micrograph of the two samples in Fig. 2 shows that the Rh nano-particles of $RhAl_1/SiO_2$ dispersed more homogeneously and the Rh particles size was more uniform than those of the Rh/SiO_2. The vast statistics of Rh particles size based on about 1000 particles from numbers of images for each sample, shown as inserts in Fig. 2, corroborated the above observation. The Rh particle size of the Rh/SiO_2 sample ranged from 0.4 to 6.4 nm, with an average particle size of 2.77 nm and a standard deviation of 0.86. Compared to Rh/SiO_2, the average Rh particle size of the $RhAl_1/SiO_2$ sample was smaller (2.08 nm) and the particle size distribution was narrower (from 0.4 to 4.0 with a standard deviation of 0.52). It is obvious that the addition of Al promoted the dispersion of Rh to form smaller and more uniform Rh particles. What is more important is that the fraction of edged and cornered Rh atoms in the total Rh surface increased with the decreasing of the Rh particle size [17], which means that more Rh atoms could be provided to form the active species for ethylene hydroformylation.

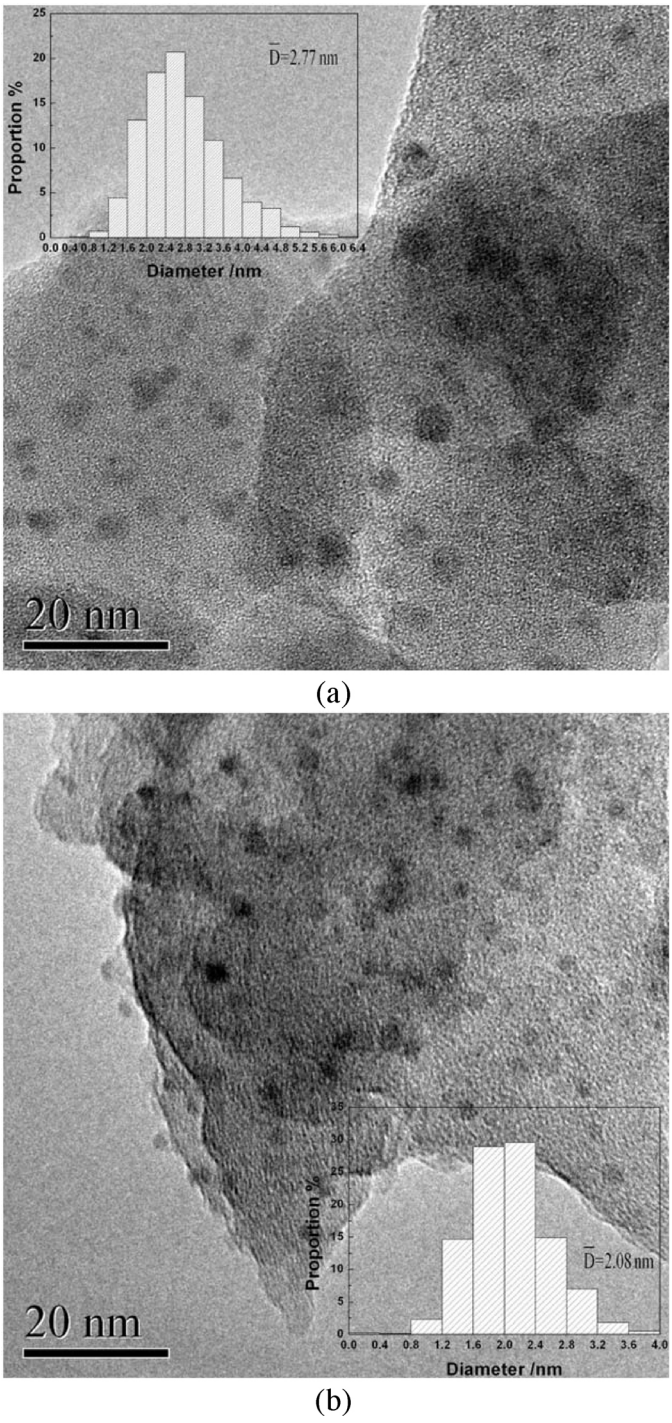

Fig. 2. TEM images of (a) Rh/SiO_2 and (b) $RhAl_1/SiO_2$. The inserts show the distribution of Rh particle size.

3.4. Pyridine adsorbed FT-IR

Since $Al(NO_3)_3{\cdot}9H_2O$ is decompounded into Al_2O_3 at 408 K [18], it should be taken into account the difference in acidity between the $RhAl_1/SiO_2$ and Rh/SiO_2 catalysts. FT-IR spectroscopy of adsorbed pyridine is a useful technique for measuring the acidity of catalysts. Fig. 3 shows the spectra of the two samples after desorption of pyridine at 423 K. Comparing the spectra between Rh/SiO_2 and $RhAl_1/SiO_2$, the band at 1446 cm^{-1} appeared in both spectra, while new bands at 1456, 1491 and 1545 cm^{-1} emerged in the spectrum of the $RhAl_1/SiO_2$. The band at 1446 cm^{-1} was attributed to pyridine adsorbed via hydrogen bonding (HB). The new bands for the $RhAl_1/SiO_2$ after pyridine desorption implied the emerging of new acid sites. The band at 1456 cm^{-1} was characterized as Lewis acid sites (LAS), the band at 1545 cm^{-1} indicated the presence of Brönsted acid sites (BAS), and the band at 1491 cm^{-1} was from the pyridine adsorbed on LAS and BAS mixtures (LBAS) [19,20]. Generally speaking, the addition of Al indubitably gave rise to the appearance of Brönsted acid sites and Lewis acid sites, which would change greatly the acidity of the catalyst surface. It has been substantiated that Lewis acid sites could accelerate the rate of CO insertion when using alkyl (pentacarbonyl) manganese [21].

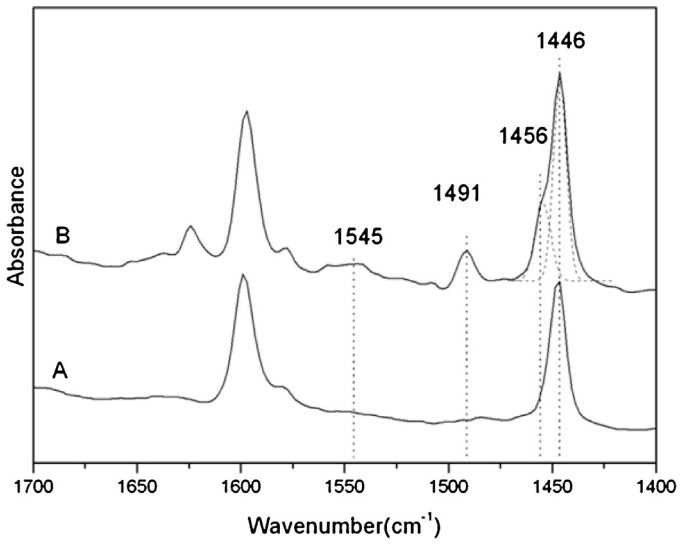

Fig. 3. Infrared adsorption spectra of adsorbed pyridine after 30 min desorption at 423 K for (A) Rh/SiO_2 and (B) $RhAl_1/SiO_2$.

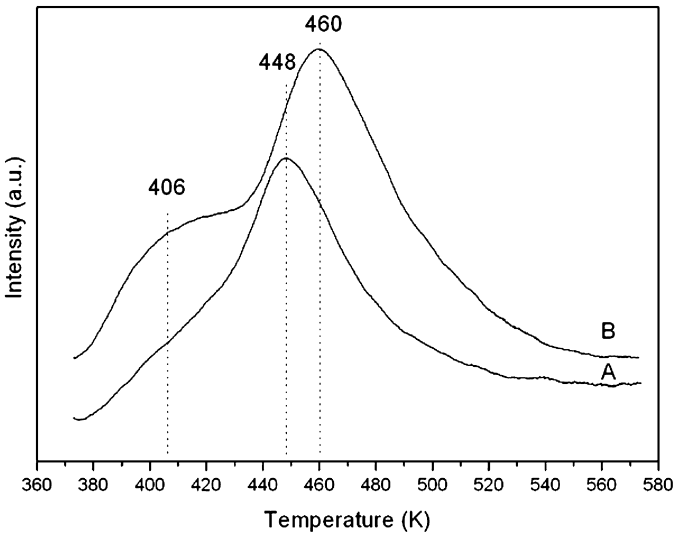

Fig. 5. NH_3-TPD profile of (A) Rh/SiO_2 and (B) $RhAl_1/SiO_2$.

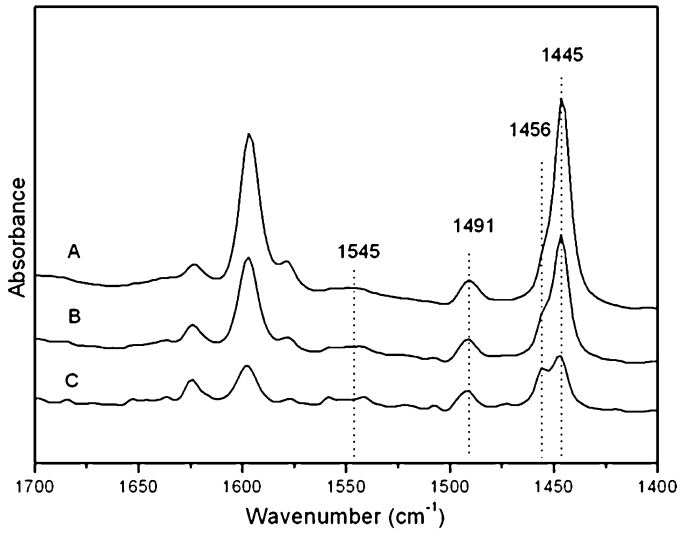

Fig. 4. Infrared adsorption spectra of pyridine adsorbed on $RhAl_1/SiO_2$ after 30 min desorption at (A) room temperature, (B) 423 K, and (C) 523 K.

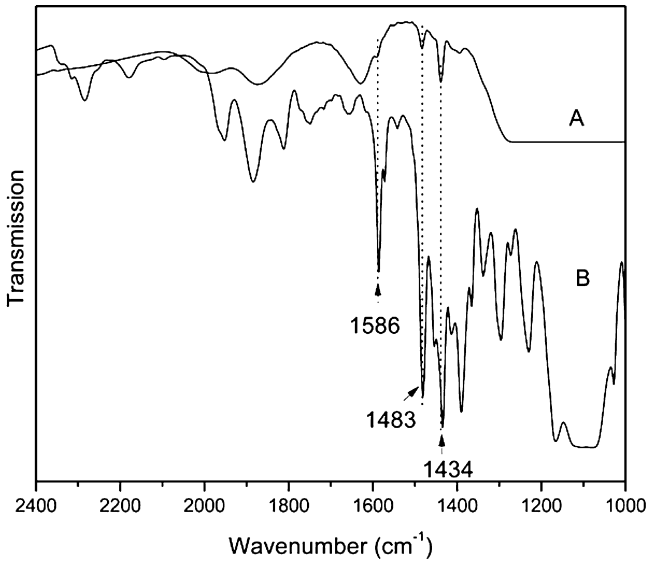

Fig. 6. FT-IR spectra for (A) DPPPTS-$RhAl_1/SiO_2$ and (B) DPPPTS.

Therefore, the appearance of LAS over $RhAl_1/SiO_2$ might be one of the factors that promoted the activity of the DPPPTS-$RhAl_1/SiO_2$ catalyst.

The effect of the acidic strength of HB, LAS, BAS on $RhAl_1/SiO_2$ was investigated by the spectra of pyridine desorption at various temperatures, as shown in Fig. 4. With the increase of the temperature from room temperature to 523 K, the intensity of the bands decreased sharply, implying that most of the acid sites were weak sites.

3.5. NH_3-TPD

NH_3-TPD is another technique suitable for characterizing the acidity of $RhAl_1/SiO_2$ and Rh/SiO_2. Fig. 5 demonstrates the spectra of ammonia desorption, which was carried out in the range of 373–573 K, as the maximum treatment temperature for the catalysts was 573 K. The acid sites were found to be weak in this temperature range. The Rh/SiO_2 gave only one peak at 448 K, while the $RhAl_1/SiO_2$ showed two new peaks at 406 and 460 K. Considering the results in the section of pyridine adsorption FT-IR, the peaks at 448, 406 and 460 K were attributed to HB, BAS and LAS, respectively. The peak areas of the $RhAl_1/SiO_2$ (2.27) and Rh/SiO_2 (1.65) suggested that $RhAl_1/SiO_2$ had a larger amount of weak acid sites than the Rh/SiO_2. The higher number of weak acid sites favored catalytic activity of olefin hydroformylation on the catalysts, according to the investigation by Kontkanen et al. [22].

3.6. FT-IR

To identify whether the DPPPTS was tethered to the SiO_2 or not, FT-IR spectroscopy was carried out. Fig. 6 shows the FT-IR spectra of the DPPPTS-$RhAl_1/SiO_2$ and DPPPTS. The DPPPTS-$RhAl_1/SiO_2$ sample displayed characteristic bands of DPPPTS at 1434 cm^{-1} (P-CH_2 vibration) [6], 1483 and 1586 cm^{-1} (C–C stretching peaks in the phenyl ring) [23], confirming the presence of DPPPTS on the DPPPTS-$RhAl_1/SiO_2$. The DPPPTS tethered on SiO_2 was referred to as DPPPTS-SiO_2.

To explain the great difference in activities between the DPPPTS-$RhAl_1/SiO_2$ and DPPPTS-Rh/SiO_2, in situ FT-IR spectra have been recorded to investigate the active species of the two catalysts, as shown in Fig. 7. After treated with a premixed gas

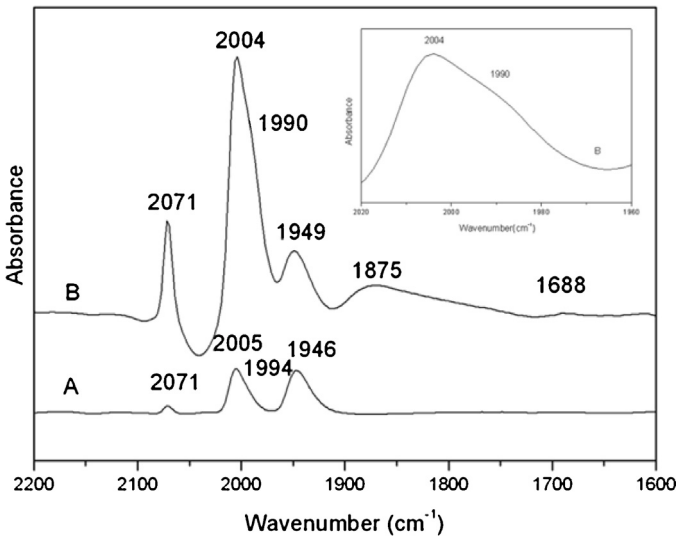

Fig. 7. In situ FT-IR of (A) DPPPTS-Rh/SiO_2 and (B) DPPPTS-$RhAl_1$/SiO_2 catalysts treated with CO:H_2 = 1:1 at atmospheric pressure and 323 K for 30 min.

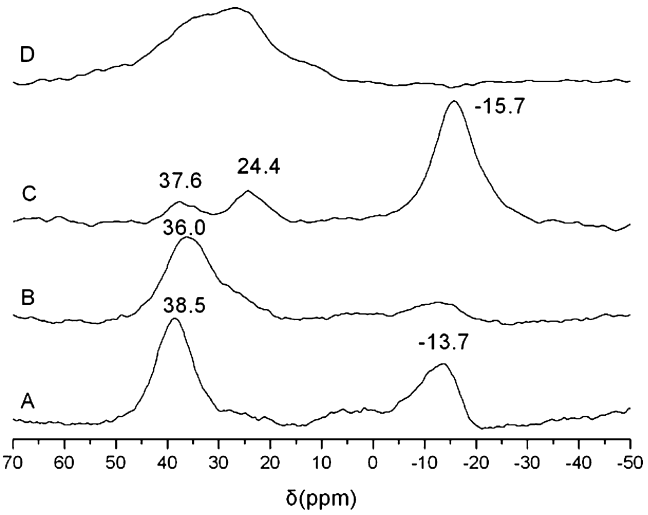

Fig. 8. ^{31}P NMR spectra of (A) fresh DPPPTS-Rh/SiO_2, (B) used DPPPTS-Rh/SiO_2, (C) fresh DPPPTS-$RhAl_1$/SiO_2, and (D) used DPPPTS-$RhAl_1$/SiO_2.

(CO:H_2 = 1:1), four bands at 2071, 2005, 1994 and 1949 cm^{-1} appeared in the spectrum of DPPPTS-Rh/SiO_2, while there were six bands at 2071, 2004, 1990, 1949, 1875 and 1688 cm^{-1} in the spectrum of the DPPPTS-$RhAl_1$/SiO_2. The bands in the range of 2071–1949 cm^{-1} were identical to those observed for soluble $HRh(CO)_2(PPh_3)_2$, $HRh(CO)_2$(xantphos), $HRh(CO)_2$(thixantphos) and SILP $HRh(CO)_2$(sulfoxantphos)/SiO_2. The bands at 2071 and 1992 ± 2 cm^{-1} were assigned to *ee*-$HRh(CO)_2$(DPPPTS-SiO_2)$_2$, whereas the bands at 2004 ± 2 and 1947 ± 2 cm^{-1} were assigned to *ea*-$HRh(CO)_2$(DPPPTS-SiO_2)$_2$ [24,25]. It is noteworthy that the intensity of the peaks in the spectrum of the DPPPTS-$RhAl_1$/SiO_2 was stronger than those in the spectrum of the DPPPTS-Rh/SiO_2. As the intensity of the peaks was proportional to the concentration of the species, it illustrated that there were more $HRh(CO)_2$(DPPPTS-SiO_2)$_2$ species on the DPPPTS-$RhAl_1$/SiO_2 catalyst than on the DPPPTS-Rh/SiO_2 catalyst. Since $HRh(CO)_2$(DPPPTS-SiO_2)$_2$ was analogous to $HRh(CO)_2(PPh_3)_2$, which is assumed to be the active species for the Wilkinson-type hydroformylation catalysts in hydroformylations [26], it was deduced that the in situ formed $HRh(CO)_2$(DPPPTS-SiO_2)$_2$ on the surface of the DPPPTS-$RhAl_1$/SiO_2 and DPPPTS-Rh/SiO_2 catalyzed the hydroformylation of ethylene. Hence, as larger amount of $HRh(CO)_2$(DPPPTS-SiO_2)$_2$ was formed in situ due to the promoting effect of Al, the DPPPTS-$RhAl_1$/SiO_2 exhibited a far higher activity than the DPPPTS-Rh/SiO_2.

Furthermore, in the FT-IR spectrum of the DPPPTS-$RhAl_1$/SiO_2, the band at 1875 cm^{-1} due to bridged CO on metallic Rh [13,27] and the small band at 1688 cm^{-1} due to a tilted CO species bound to Rh, in which the oxygen atom interacted with the Lewis acid sites [28], indicated that, besides the $HRh(CO)_2$(DPPPTS-SiO_2)$_2$ species, there existed exposed Rh atoms not modified by phosphine ligands on the DPPPTS-$RhAl_1$/SiO_2 catalyst. Consequently, Al favored the in situ formation of the $HRh(CO)_2$(DPPPTS-SiO_2)$_2$ species and prompted the amount of exposed Rh atoms, both of which could enhance the activity towards hydroformylation.

3.7. Solid-state ^{31}P NMR

Further evidence for species formed in situ on the catalysts was obtained by solid-state ^{31}P NMR spectroscopy characterization. Fig. 8 displays the ^{31}P NMR spectra of fresh and used DPPPTS-Rh/SiO_2 and DPPPTS-$RhAl_1$/SiO_2. The spectrum of fresh DPPPTS-Rh/SiO_2 showed two bands at −13.7 and 38.5 ppm, the former band was ascribed to free DPPPTS-SiO_2 and the latter band to DPPPTS-SiO_2 coordinated with Rh [6,29,30]. In the used DPPPTS-Rh/SiO_2, the band at −13.7 ppm attenuated, whereas the band at 38.5 ppm shifted upfield to 36.0 ppm. The band at 36.0 ppm was assigned to the Wilkinson-type catalyst tethered on silica gel, which was caused by interaction between the catalyst and the reaction gas [23]. In contrast, there were three broad bands at −15.7, 24.4 and 37.6 ppm in the spectrum of the fresh DPPPTS-$RhAl_1$/SiO_2. Similar to the bands at −13.7 and 38.5 ppm on DPPPTS-Rh/SiO_2, the bands at −15.7 and 37.6 ppm on DPPPTS-$RhAl_1$/SiO_2 were assigned to free DPPPTS-SiO_2 and coordinated DPPPTS-SiO_2, respectively, the small difference in chemical shift was due to the change in chemical environment of P. The new band at 24.4 ppm implied a third kind of DPPPTS species, which was uncharacterized because the region of 20–34 ppm was also occupied by other phosphorus compounds such as phosphine oxides and phosphonic and phosphinic acids [31]. As for the used DPPPTS-$RhAl_1$/SiO_2, the free DPPPTS-SiO_2 band disappeared and a very broad band at the region of 7.3–46.7 ppm, which might be due to the overlap of several active species bands, emerged. The chemical environment of P in the solid-state ^{31}P NMR spectra of used DPPPTS-$RhAl_1$/SiO_2 was not the same as that of the used DPPPTS-Rh/SiO_2 catalyst. The disappearance of free DPPPTS-SiO_2 over the two catalysts and the growing TOF numbers in Fig. 1 manifested that free DPPPTS-SiO_2 was gradually transformed into coordinated DPPPTS-SiO_2 with Rh to the in situ formed $HRh(CO)_2$(DPPPTS-SiO_2)$_2$ species during hydroformylation.

3.8. Solid-state ^{27}Al NMR

The only difference of the two catalysts was the existence of Al in DPPPTS-$RhAl_1$/SiO_2. Therefore, ^{27}Al NMR was carried out to seek assignment for the band at 24.4 ppm in the solid-state ^{31}P NMR spectrum of the fresh DPPPTS-$RhAl_1$/SiO_2. As shown in Fig. 9, $RhAl_1$/SiO_2 displayed two bands at 2.7 and 53.3 ppm, attributed to Al^{VI} and Al^{IV}, respectively [19]. After DPPPTS was tethered to $RhAl_1$/SiO_2, the band at 2.7 ppm shifted upfield to −8.9 ppm, implying that DPPPTS enhanced electron screening of Al^{VI}.

Combining the results of solid-state ^{31}P NMR with that of ^{27}Al NMR, it is clear that there were some interactions between ligand-modified Rh and Al. Given the upfield shift of Al, an electron-donating group of Al–O^-–Al might directly or indirectly act on P in the phosphine ligand and gave the band at 24.4 ppm in ^{31}P NMR. There are two possible modes of interaction: one is that O^- gives electrons to P and conduces higher electron density of P, the other

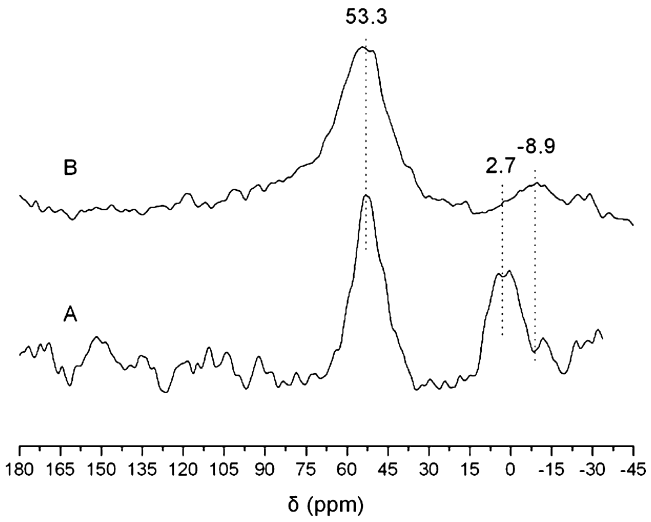

Fig. 9. ^{27}Al NMR spectra of (A) $RhAl_1/SiO_2$ and (B) $DPPPTS\text{-}RhAl_1/SiO_2$.

is that O^- coordinates with Rh with electrons transferring to P through the Rh–P bond. In both modes, the phenyl of the phosphine could interact with Al due to the short space distance, and caused the enhancement of Al^{VI} electron screening. Further studies are in progress in our laboratory.

4. Conclusion

The promoting effect of Al on a tethered ligand-modified Rh/SiO_2 catalyst for hydroformylation is very inspiring. The activity for ethylene hydroformylation of a tethered ligand-modified Rh/SiO_2 catalyst with Al doping was 4 times as high as that without Al. The promoting effect of Al can be summarized into three aspects: (1) it increased the number of exposed Rh atoms and inhibited the growth of the Rh particles; (2) it changed the acidity of the catalyst surface; and (3) it promoted the in situ formation of the active species of $HRh(CO)_2(DPPPTS\text{-}SiO_2)_2$. Furthermore, the new peak at 24.4 ppm of the ^{31}P NMR and the band at 2.7 ppm shifted upfield to −8.9 ppm in the ^{27}Al NMR spectra indicated that Al also interacted with the tethered DPPPTS. Our results indicate that promoters can open up new ways to improve the activities of tethered ligand-modified Rh catalysts.

Acknowledgment

This work was supported by NSFC (21273227 and 20903090).

References

[1] A.C.J. Koeken, N.M.B. Smeets, Catal. Sci. Technol. 3 (2013) 1036–1045.
[2] X. Feng, G.E. Fryxell, L.Q. Wang, A.Y. Kim, J. Liu, K.M. Kemner, Science 276 (1997) 923–926.
[3] P. Mastrorilli, C.F. Nobile, Coord. Chem. Rev. 248 (2004) 377–395.
[4] Z.M. Michalska, Ł. Rogalski, K. Rózga-Wijas, J. Chojnowski, W. Fortuniak, M. Ścibiorek, J. Mol. Catal. A: Chem. 208 (2004) 187–194.
[5] C. Jones, M. McKittrick, J. Nguyen, K. Yu, Top. Catal. 34 (2005) 67–76.
[6] X. Li, Y. Ding, G. Jiao, J. Li, R. Lin, L. Gong, L. Yan, H. Zhu, Appl. Catal. A 353 (2009) 266–270.
[7] H.W. Jen, Y. Zheng, D.F. Shriver, W.M.H. Sachtler, J. Catal. 116 (1989) 361–372.
[8] K. Tomishige, I. Furikado, T. Yamagishi, S. Ito, K. Kunimori, Catal. Lett. 103 (2005) 15–21.
[9] A. Trunschke, H.C. Böttcher, A. Fukuoka, M. Ichikawa, H. Miessner, Catal. Lett. 8 (1991) 221–228.
[10] S.S.C. Chuang, S.-I. Pien, J. Catal. 138 (1992) 536–546.
[11] S.S.C. Chuang, G. Srinivas, M.A. Brundage, Energy Fuel 10 (1996) 524–530.
[12] Y.J. Kim, J.B. Joo, H.C. Kim, J. Yi, J. Nanosci. Nanotechnol. 10 (2010) 269–274.
[13] J.M. Coronado, F. Coloma, J.A. Anderson, J. Mol. Catal. A: Chem. 154 (2000) 143–154.
[14] J. Wrzyszcz, M. Zawadzki, A. Trzeciak, W. Tylus, J. Ziółkowski, Catal. Lett. 93 (2004) 85–92.
[15] M. Lenarda, R. Ganzerla, S. Enzo, L. Storaro, R. Zanoni, J. Mol. Catal. 80 (1993) 105–116.
[16] M. Capka, Syn. React. Inorg. Metal Org. Chem. 7 (1977) 347–354.
[17] H. Arakawa, N. Takahashi, T. Hanaoka, K. Takeuchi, T. Matsuzaki, Y. Sugi, Chem. Lett. 17 (1988) 1917–1918.
[18] N. Lange, J. Dean, Lange's Chemistry Handbook Version 15th, McGraw-Hill Professional, Knoxville, TN, 1999.
[19] C. Hernandez, A.C. Pierre, Langmuir 16 (1999) 530–536.
[20] J.H. Ahn, R. Kolvenbach, C. Neudeck, S.S. Al-Khattaf, A. Jentys, J.A. Lercher, J. Catal. 311 (2014) 271–280.
[21] S.C. Chuang, R. Stevens Jr., R. Khatri, Top. Catal. 32 (2005) 225–232.
[22] M.-L. Kontkanen, M. Tuikka, N. Kinnunen, S. Suvanto, M. Haukka, Catalysts 3 (2013) 324–337.
[23] K. Bogár, P. Krumlinde, Z. Bacsik, N. Hedin, J.-E. Bäckvall, Eur. J. Org. Chem. 2011 (2011) 4409–4414.
[24] S. Shylesh, D. Hanna, A. Mlinar, X.-Q.n. Kŏng, J.A. Reimer, A.T. Bell, ACS Catal. 3 (2013) 348–357.
[25] A. Riisager, R. Fehrmann, S. Flicker, R. van Hal, M. Haumann, P. Wasserscheid, Angew. Chem. Int. 44 (2005) 815–819.
[26] C.K. Brown, G. Wilkinson, J. Chem. Soc. A (1970) 2753–2764.
[27] G. Srinivas, S.S.C. Chuang, J. Catal. 144 (1993) 131–147.
[28] C.P. Horwitz, D.F. Shriver, C- and O-bonded metal carbonyls: formation, structures, and reaction, in: F.G.A Stone, W. Robert (Eds.), Adv. Organomet. Chem., Academic Press, 1984, pp. 219–305.
[29] C. Merckle, J. Blümel, Chem. Mater. 13 (2001) 3617–3623.
[30] J.-R. Chang, H.-M. Lin, S.-W. Cheng, C.-K. Tseng, D.-L. Tzou, S.-G. Shyu, J. Mol. Catal. A: Chem. 329 (2010) 27–35.
[31] J. Sommer, Y. Yang, D. Rambow, J. Blümel, Inorg. Chem. 43 (2004) 7561–7563.